# Lawrence Berkeley Laboratory
UNIVERSITY OF CALIFORNIA



Presented at the XI Nuclear Physics Symposium,
Oaxtepec, Mexico, January 4–7, 1988, and to
be published in the Proceedings

## Capture Reactions of $^{40}Ca$ and $^{48}Ca$ with Targets of $^{197}Au$ and $^{208}Pb$

R. Stokstad, Y. Chan, E. Chavez, D. Di Gregorio,
M. di Tada, S. Gazes, J. Fernandez-Niello, A. Pacheco,
E. Plagnol, and J. Testoni

March 1988

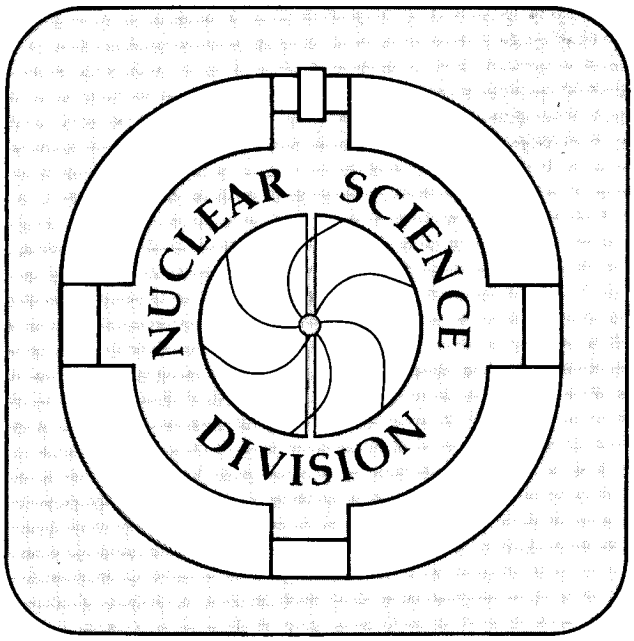


Prepared for the U.S. Department of Energy under Contract DE-AC03-76SF00098

## DISCLAIMER

# Capture Reactions of $^{40}Ca$ and $^{48}Ca$ with Targets of $^{197}Au$ and $^{208}Pb$

R. Stokstad[a], Y. Chan[a], E. Chavez[a,b], D. Di Gregorio[c], M. di Tada[c], S.Gazes[a,d], J. Fernandez-Niello[c], A. Pacheco[c], E. Plagnol[a,e], and J.Testoni[c]

a) Nuclear Science Division, Lawrence Berkeley Laboratory, Berkeley, CA 94720
University of California
b) Instituto de Fisica, Universidad Nacional Autonoma Mexico, A.P. 20-364, Mexico

c) Departamento de Fisica, Comision Nacional de Energia Atomica, 1429 Buenos Aires

d) Present address: Department of Physics, University of Rochester, Rochester, NY 14627

e) On leave from Institut de Physique Nucleaire, Orsay

## ABSTRACT

The reactions of $^{40}Ca$ and $^{48}Ca$ with targets of $^{197}Au$ and $^{208}Pb$ have been measured in the region from below the interaction barrier to about twice the barrier energy. The fission-like fragments were detected in a pair of position-sensitive, multi-wire proportional counters and were identified from measurements of position and time using two-body kinematics. In the region above the barrier the cross sections for capture are less than those given by the touching condition, indicating that an "extra push" is required to induce capture. The observations for $^{40}Ca$ and $^{48}Ca$ show different fissilities for the onset of the extra push and indicate that charge equilibration may be an important factor governing capture reactions. Below the barrier the cross sections show an enhancement relative to the prediction for a one dimensional barrier. The enhancements are larger for $^{40}Ca$ than for $^{48}Ca$ (for both targets) and this is in qualitative agreement with predictions based on the coupling of the relative motion to low-lying collective states. Both above and below the barrier, we find that the change in the light partner, from $^{48}Ca$ to $^{40}Ca$, has a larger effect on the cross sections than the change from $^{208}Pb$ to $^{197}Au$, after correction for the change in the Coulomb barrier.

## I. Introduction

The study of fusion reactions or, more generally, capture reactions with heavy ions has revealed an interesting and rich interplay of nuclear structure and reaction mechanism. Basically, the barrier for fusion governs the size and energy dependence of the cross section. Nuclear structure, both on a macroscopic and microscopic level, determines the barrier. The macroscopic aspects (Coulomb repulsion, liquid-drop-like nuclear forces, moments of inertia) set the global behavior. For example, when the colliding nuclei are highly charged, fusion at

the barrier is inhibited and extra energy is required to force the nuclei together. On top of these first-order effects come interesting second order effects. In the case of very heavy nuclei, it appears that shell effects can influence cross sections at bombarding energies above the barrier. [Ar86] The second-order effects, which can be greatly magnified if the bombarding energy is well below the barrier, are intimately connected with nuclear structure and arise from collective nuclear phenomena -- deformation and vibration -- and from microscopic, individual-particle properties -- nucleon transfer. The reader is referred to an excellent review by Reisdorf that presents these aspects of heavy-ion fusion in more detail. [Re86]

Basic to an understanding of these processes are measurements that can single out or isolate particular effects for study. Thus, the effect of deformation is examined by comparing targets that are otherwise similar except for their deformation. The isotopes of samarium are a prime example. [St80, Di86] Similarly, the tin nuclei are excellent for studying the effects of vibration.[Re85, Ja86] It is also of interest to examine cases in which the effects of nuclear structure (the rotations and vibrations mentioned above) are minimized. This should help test our understanding of the underlying nuclear potential that is the basis for the one-dimensional calculations of nuclear fusion. Reactions of doubly-magic projectile and target nuclei are the closest approximation we have to this ideal situation, and we have chosen the systems $^{40,48}Ca + ^{208}Pb$ for study.

A second factor influencing the choice of projectile and target in the present work is the threshold at which the extra push becomes important. Expressed in terms of an effective fissility, $x'_{Bass}$, this threshold is known to lie in the vicinity of projectile-target combinations like Ca + Pb, and has a value of ~0.7. [To 85] The availability of the projectiles $^{40}Ca$ and $^{48}Ca$ enables one to vary the effective fissility in the region of the extra-push threshold without the large change in barrier height accompanying a change in projectile charge. Thus, we have undertaken an experimental study of the capture reactions of $^{40,48}Ca$ on targets of $^{197}Au$ and $^{208}Pb$ at energies above and below the barrier. In the following we report results that are preliminary in that only a portion of the total amount of experimental data has been analyzed so far. Values of the cross sections may change somewhat as measurements at additional scattering angles are processed. Nevertheless, we expect that the present results are sufficient to demonstrate the major trends in the experimental data.

## II. Experimental arrangement

Beams of $^{40}Ca$ and $^{48}Ca$ were obtained from the LBL ECR ion source and 88-Inch Cyclotron. The targets were self-supporting thin foils of Au or isotopically enriched $^{208}Pb$ and had thicknesses of 200-250 $\mu gm/cm^2$. A surface barrier detector located at 11.8° and above

the reaction plane was used to monitor the Rutherford scattering from the target, and thereby provide a normalization for the absolute cross section.

The heavy reaction products were detected in coincidence in a pair of multi-wire proportional counters, each with an active area of 16x16 $cm^2$, as shown in Fig. 1. These counters were positioned at angles of $30^o$ and $110^o$, where the first angle is that of the master detector, at every bombarding energy and at additional angles of 55/60, 55/80, and 80/55 degrees at selected bombarding energies. A measurement of the position coordinates of each fragment and the difference in time-of-arrival of the fragments at each detector is sufficient to determine all the parameters of a reaction having only two heavy bodies in the final state. In practice, the time difference by itself is practically sufficient to identify the fission fragments. This is illustrated in Fig. 2, which shows the time difference versus the anode signal in the master detector. If the reaction is indeed binary, then the fragments must lie in one plane. A measurement of the coplanarity in the lab system (colinearity in the c.m. system) of the two fragments provides an independent check on the binary nature of the reaction. The coplanarity is illustrated in Fig. 3a. Even up to the highest bombarding energies (~ 10 MeV/A) we found little evidence for non-binary reactions involving three heavy fragments.

## III. Data Reduction

The reduction and analysis of the experimental data have been done in Buenos Aires at the TANDAR facility. The data were analyzed event by event using absolute position and time calibrations. These calibrations were checked against the elastic scattering. The mass distributions and total kinetic energies of the fragments for the reaction $^{48}Ca + ^{208}Pb$ at $E_{c.m.}$ = 205 MeV are illustrated in Figs. 3b and 3c. The mass distribution peaks at symmetry and its centroid is independent of bombarding energy. Its width (standard deviation) increases gradually from 23 to 29 a.m.u. as the bombarding energy increases from the interaction barrier to the highest energy, 338 MeV. This behavior is similar to that observed for the reactions $^{26}Mg$ and $^{27}Al$ with $^{238}U$. [Sh87] These widths are at or slightly larger than the values expected for equilibrium fission.

The total kinetic energy loss (TKEL) spectrum shown in Fig. 3c includes all masses shown in Fig. 3b and it is thus not possible to make a precise comparison with the systematics of Viola [Vi85], which are for symmetric fission. Until all the projectile-target combinations have been analyzed for all the bombarding energies, we will have to reserve judgement on how closely the present experimental data fit the systematics of equilibrium fission. However, this preliminary analysis suggests that the reaction products observed here have the characteristics typical of fission or quasifission reactions in this mass region. [Sh87]

## IV. Cross Sections

Absolute cross sections for the fission-like component of the yield were obtained in the following manner. After converting the laboratory coordinates for each event to the center of mass, a region of scattering angle in the master detector, $38^{o}$ - $43^{o}$ c.m., was selected on the basis that the slave detector detected, at a single position, each partner in coincidence with a fission-like fragment in this particular angular region. This holds for fragments in the master detector with masses both above and below symmetry (128 a.m.u.). In this way an absolute center-of-mass differential cross section was obtained. The angular distribution for equilibrium fission [Ba85], which depends on the quantities I and $K_o^2$, was then calculated by interpolating values for I and $K_o^2$established in other experiments. [Sh87] It turns out that this particular angular range near $40^{o}$ is one for which the different angular distributions (for different values of I and $K_o^2$) tend to coincide. As a consequence, the conversion from differential to angle-integrated cross section is not particularly sensitive to the parameters determining the theoretical angular distribution. In the following, absolute values are based on measurements made with the $30^{o}/110^{o}$ settings of the master and slave detectors. Any asymmetric contributions to the angular distribution from quasi-fission will cause us to overestimate the angle-integrated cross section. However, examination of the detailed angular distributions measured for $^{27}Al + ^{238}U$ suggest that any such effects will be small. [Sh87]

Absolute cross sections as a function of bombarding energy are shown in Fig. 4 for the four systems measured. The linear scale better displays the cross sections above the barrier. (The subbarrier dependence is shown in Fig. 7. in a semi-logarithmic plot.) The cross sections for capture measured in this work span the range from a few to a thousand millibarns.

## V. The Above-Barrier Results: the Extra Push

If the attractive nuclear force dominates the Coulomb and centrifugal forces, as in the case of lighter projectiles such as $^{16}O$, then the capture cross section is given by the relation

$$\sigma = \pi R^2_{int} (1-V_{int}/E)$$

where $V_{int}$ and $R_{int}$ are the interaction barrier and radius, respectively. In light systems capture leads directly to fusion. In heavier systems, capture not leading to fusion produces fission-like reaction products whose characteristics are difficult to distinguish from fusion-fission. This cross section, associated with the touching condition, $r=R_{int,}$ is shown in Fig. 4 for the indicated values of $V_{int}$ and $R_{int}$. (These have been calculated following the procedure given by Toke, et al. and using the exponential parametrization for the proximity function $\phi(r)$ given by Blocki, et al.[To85, Bl77]) Once the bombarding energy is 20-30 MeV above the interaction barrier, the experimental capture cross section, $\sigma_c$ , deviates substantially, becoming

progressively lower as the bombarding energy increases. The deviation between the experimental values and the touching cross section can be expressed in terms of the extra energy $E_x$ (or "push") needed to induce capture relative to the energy needed if the touching condition were sufficient to induce capture. Thus, the definition:

$$E_t \, \sigma_t(E_t) = \pi\hbar^2 L_c^2/2\mu = E_c \, \sigma_c(E_c)$$

which enables the experimental values of the extra-push energy $E_x$ to be determined from the data using the relation $E_x = E_c - E_t$.

A dynamical theory of heavy ion reactions developed by Swiatecki makes it possible to predict the magnitude and energy dependence of $E_x$. [Sw81] In practice, the values of the (relatively few) parameters in the theory are determined by comparison with experiment. The measure of the theory then is its ability to predict, or scale, a wide range of experimental results with one set of parameters determined from a global fit to experiment. Based mainly on the extensive measurements carried out in recent years at the GSI using projectiles of $^{208}Pb$ and $^{238}U$, [To85, Sh87] such a systematic study and analysis have been done. Accordingly, we follow the procedures described by Toke, et al., and by Shen et al., in the analysis of our results. In Fig. 5 the values of $\sqrt{E_x}$ are plotted as a function of $L^2$ (essentially, the cross section times the energy). The scaling parameters $E_{ch}$ and $L_{ch}$ given by the theory compress a wide range of experimental results into a smaller, dimensionless space.The result of the extra-push theory is expressed as

$$(E_x/E_{ch})^{1/2} = a(x'_{Bass}(0) - x'_{th}) + a\, f^2(L_c/L_{ch})^2$$

where the slope parameter a is a constant with a value of about 10, $x'_{Bass}$ is the effective fissility ( the ratio of the Coulomb and nuclear forces for L=0), $x'_{th}$ is the threshold fissility for the extra push, and f is the fraction of angular momentum remaining in orbital motion after the nuclei interact. (See Toke et al. for a complete discussion). The results in Fig. 4 are recast in Fig. 5 in the dimensionless quantities of the extra-push theory. Also show in Fig. 5 are the predictions based on the parameters for a=10, $x_{th}$ =0.7 and f=0.65 determined by Toke, et al. Note that good agreement with the theory is obtained for the case of the $^{48}Ca$ beam on both the Au and Pb targets. There is a rather striking discrepancy for $^{40}Ca$, however. In these cases a much higher value for the extra-push energy is predicted (at a given value of $L^2$) than is observed experimentally. Note that the situation is the same for Au and Pb targets. It is in this sense we say that it is the change in the nature of the lighter partner (from $^{48}Ca$ to $^{40}Ca$ ) rather than in the target (Au or Pb) that is the determining factor in the observed differences.

The value of $E_x$ for a central collision can be determined from the data in Fig. 5 and plotted as a function of the effective fissility of the system. (In extrapolating the experimental data to

L=0, we use only the higher energy points, which are sufficiently above the barrier so as to be uninfluenced by barrier fluctuations, i.e. , by the nuclear structure effects to be discussed in the next section.) In Fig. 6 these intercepts are shown for the present work and the systems studied by Toke, et al. The results of Figs. 5 and 6 indicate that the reactions induced by $^{40}Ca$ have a higher threshold fissility for the extra push associated with them than $^{48}Ca$. This result depends, of course, on the scaling parameter $x'_{Bass}$. The situation changes if a different scaling parameter, $(x'_{Bass})_{eq}$, is used, as has been pointed out by Shen, et al. [Sh87]. This parameter assumes a rapid charge-to-mass equilibration at the touching configuration (i.e., for fixed mass asymmetry). For a target of $^{208}Pb$ and projectiles of [$^{40}Ca$ , $^{48}Ca$] we have ,respectively, $x'_{Bass}$ = [0.75, 0.70] and $(x'_{Bass})_{eq}$ = [0.64, 0.67]. Using a charge-equilibrated scaling would reverse the situation and have the $^{48}Ca$ projectile exhibit a higher threshold fissility. Thus, the aspect of charge equilibration [Sh87] seems to be important when examining in detail the small but nevertheless significant deviations between experiment and the systematic behavior predicted by the extra-push model. Indications for deviations involving other doubly-magic heavy collision partners also have been presented. [Ar86] It seems that the closer one looks the more complicated the situation appears - a characteristic of nuclear physics, and science in general!

## VI. Below the Barrier: Channel Coupling

The experimental results at the lower bombarding energies are shown in Fig. 7. The energy scale is relative to the fusion barrier as determined by Bass [Ba74], and the particular value of the barrier is indicated on the figure. (Note that the highest energy data points do not appear on these plots.) Fig. 7a compares the excitation functions for $^{40}Ca$ and $^{48}Ca$ for the Au target, and Fig. 7c is the same but for the Pb Target. In each case, a line to guide the eye has been drawn for the $^{40}Ca$ excitation function. In the region above 1.1 times the barrier, the data (as shown on a semi-log plot) are quite similar. Below the barrier, however, deviations are apparent. Note in both cases (Figs. 7a and 7b) that the excitation function for $^{48}Ca$ falls more steeply. There does not seem to be any such difference associated with the target: that is, the excitation functions for $^{40}Ca$ on Pb and on Au overlap when plotted relative to their barriers.

The subbarrier cross sections represent a combination of 1) equilibrium fission following compound nucleus formation and 2) the capture of the reaction partners to form a di-nuclear system in which the mass asymmetry and the kinetic energy degrees of freedom have equilibrated. It is likely that most of the cross section corresponds to 2) rather than 1). The capture process represents a doorway to the formation of a system that is quite different from the entrance channel, and the process is governed by a barrier. Thus it seems reasonable to

treat the barrier fluctuation problem for capture in the same manner as it is done for reactions in which the passing of the barrier leads solely to fusion. The effect of the dynamical hindrance for capture at energies above the barrier (the need for an extra push) is harder to evaluate quantitatively for subbarrier energies. The extra-push energy is positive only for the larger partial waves that are important at higher bombarding energies. In this sense it should not influence the cross section below the barrier. On the other hand, there is a broad distribution of l-values in the entrance channel that lead to capture, even below the barrier. [Da85, Re86]

It is interesting to see to what extent these results for doubly-magic nuclei may be understood at least qualitatively in terms of the coupling of the relative motion in the entrance channel to the collective degrees of freedom of the interacting nuclei. Dasso, et al. have shown how this coupling to other channels results in an effective splitting of a single barrier into two barriers (for each coupled channel.[Da83] In the subbarrier region, where penetrabilities vary rapidly with the energy available with respect to the effective barrier, the lower barrier dominates and results in an enhanced cross section. These barrier fluctuations can be related directly to the known (or estimable) nuclear structure properties of the colliding nuclei, and inelastic scattering and transfer channels can be treated in the same framework. We have made calculations similar to those reported in [Da85] using the simplified coupled-channels code for fusion, CCFUS, written by Dasso and Landowne. [Da86] Fig. 7b shows the cross section without coupling, with the one- and two-neutron transfer channels included, and with the excitation of the low-lying $2^+$ and $3^-$ states of projectile and target included. The neutron transfer channels do not contribute much relative to the inelastic coupling, and in the case of $^{48}$Ca their contribution is negligible. Even though the couplings included in this calculation do not reproduce quantitatively the magnitude of the subbarrier enhancements, the relative predictions for $^{40}$Ca and $^{48}$Ca are of significance. For the inelastic scattering it is the greater collective multipole strength in $^{40}$Ca that causes the enhancement relative to $^{48}$Ca shown in Fig. 7d. One may also understand this difference in nuclear structure as a reflection of the greater magicity of $^{48}$Ca, i.e., some doubly-magic nuclei are more magic than others.

## VII. Summary and Outlook

Measurements of the capture reactions for projectiles of $^{40}$Ca and $^{48}$Ca with targets of $^{197}$Au and $^{208}$Pb have been made in the energy region spanning the interaction barrier. In the region above the barrier the inhibition of capture reactions - the need for an extra push - is evident. This was to be expected based on the existing systematic studies for other systems. [Sh87] When examined more closely, however, the results for $^{40}$Ca and $^{48}$Ca show inconsistencies with the predicted scaling in the vicinity of the threshold for the extra push and

suggest that charge equilibration in the early stage of the capture reaction is important. Below the barrier, $^{40}Ca$ exhibits an enhanced cross section relative to $^{48}Ca$. This may be understood qualitatively in terms of channel coupling effects and barrier fluctuations. It appears that 1) the very large difference in the neutron-to-proton (N/Z) ratio for $^{40}Ca$ and $^{48}Ca$ and 2) the strong driving potential for N/Z equilibration when nuclei of different N/Z ratio come in contact, may be connected with the different behavior of the cross sections for $^{40}Ca$ and $^{48}Ca$ both above and below the barrier.

The analysis of these experimental data is still in progress. There are measurements at additional energies and angles that will provide additional points of comparison with theory, not only for cross sections but also for mass and total kinetic energy distributions. A "first comparison" of the cross sections has been made with systematics based on the extra-push model and the experimental data obtained at the GSI. More detailed comparisons and actual fitting of our results are in progress. A unified analysis in which the dynamical hindrance above the barrier and the effects of fluctuations on capture below the barrier is needed. The present preliminary results, however, do provide a guide to the physics of these four reactions.

## Acknowledgements

We are pleased to acknowledge helpful advice from W. J. Swiatecki in the planning of the experiments and subsequent discussions. These results are a part of a collaboration between physicists in the Department of Physics at the TANDAR laboratory in Buenos Aires and physicists associated with the Nuclear Science Division at Lawrence Berkeley Laboratory. This collaboration is supported in part by grants from the CONICET and CNEA (Argentina) and from the NSF (United States) under agreement No. INT-8413645, and by the Director, Office of Energy Research, Division of Nuclear Physics of the Office of High Energy and Nuclear Physics of the U.S. Department of Energy under Contract DE-AC03-76SF00098

## References

[Ar86] P. Armbruster, Lectures given at the International School on Heavy Ion Physics , Erice, Italy, October 12-22, 1986, GSI Preprint 86-56

[Ba85] B.B. Back, et al., Phys. Rev. **C32**, 195 (1985)

[Ba74] R. Bass, Nucl. Phys. **A231**, 45 (1974)

[Bl77] J. Blocki, et al., Ann. of Phys. **105**, 477 (1977)

[Bo82] R. Bock, et al., Nucl. Phys. **A388**, 334 (1982)

[Da83] C. Dasso, et al., Nucl. Phys. **A407**, 221 (1983)

[Da86] C. Dasso and S. Landowne, Proc. Many Facets of Heavy-Ion Reactions, Argonne, 1986 ANL-PHY-86-1

[Di86] D. Di Gregorio, et al., Phys. Letts. **B176**, 322 (1986)

[Ja86] P. Jacobs, et al., Phys. Letts. **B175**, 271 (1986)

[Re85] W. Reisdorf, et al., Nucl. Phys. **A438**, 212 (1985)

[Re86] W. Reisdorf, Proc. Int. Conf. on Nuclear Physics, Harrogate, 25-30 August 1986

[Sh87] W. Q. Shen, et al., Phys. Rev. **C36**, 115 (1987)

[St80] R. G. Stokstad, et al., Phys. Rev. **C21**, 2427 (1980)

[Sw81] W.J. Swiatecki, Physica Scripta **24**, 113 (1981)

[To85] J. Toke, et al., Nucl. Phys. **A440**, 327 (1985)

[Vi85] V. Viola, Phys. Rev. **C31**, 1550 (1985)

## Figure Captions

**1.** The experimental arrangement of the MWPC's and monitor detector in the 60-inch scattering chamber. Measurements were also made at other angular configurations.

**2.** Signals from the anode of the master detector shown versus the difference in arrival time of the two fragments at a) an energy near the barrier, and b) further below the barrier.

**3.** Spectra indicating a) the coplanarity of the detected fragments, b) the mass distribution for a narrow range of angles in the center of mass, and c) the total kinetic energy loss for the entire range of masses in b).

**4.** The capture cross sections for the four reactions studied. The error on the absolute cross sections is typically 20%, while the relative errors are typically 12%-15%. The errors for the lowest bombarding energy in each case are larger, of the order of 30%. The curve is the cross section which would obtain if all partial waves exceeding the interaction barrier, $V_{int}$ , were to lead to capture.

**5.** The data of the previous figure cast in terms of the extra-push theory. The ordinate is the root of the experimentally-determined extra-push energy and the abscissa the maximum L-value leading to capture as determined by the experimental capture cross section. The scaling parameters $E_{ch}$ and $L_{ch}$ are given by the model .

**6.** The extra-push energies, extrapolated to L=0, for the four systems studied here and for those by Toke, et al. [To85]

**7.** a) and c): the present experimental results plotted so as to exhibit the behavior in the region below the barrier. b) and d): calculations of the capture cross section, which is defined as the cross section for those partial waves exceeding or penetrating the barriers determined by the coupling to excited states and transfer channels. The calculations were made with the code CCFUS [Da86].

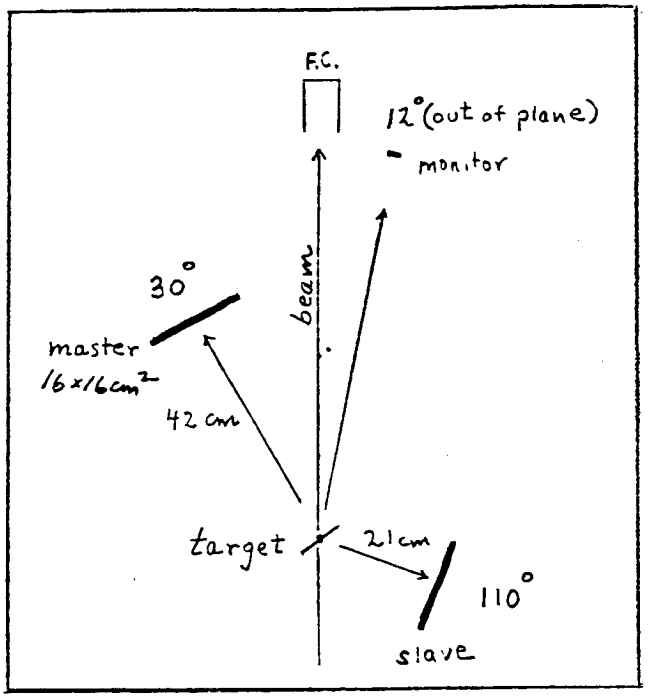


Fig. 1

Capture Reaction for $^{48}Ca + ^{208}Pb$

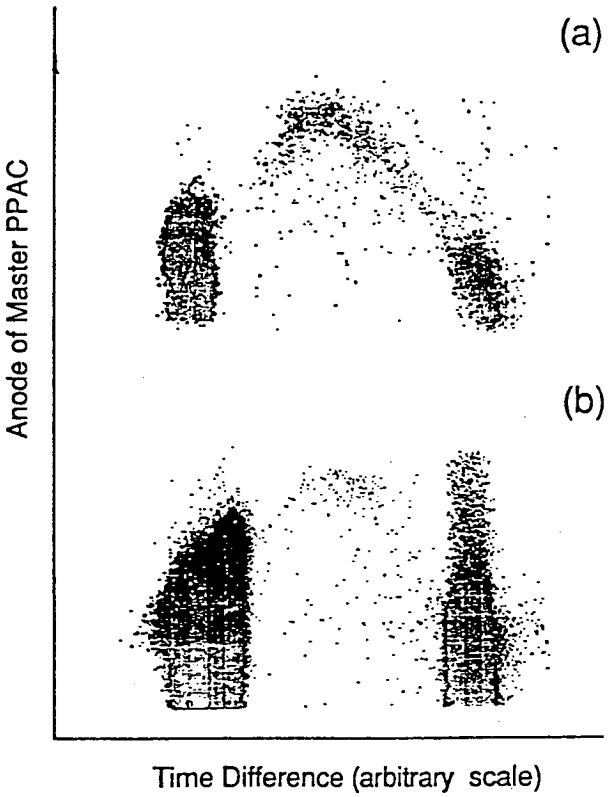


Fig. 2

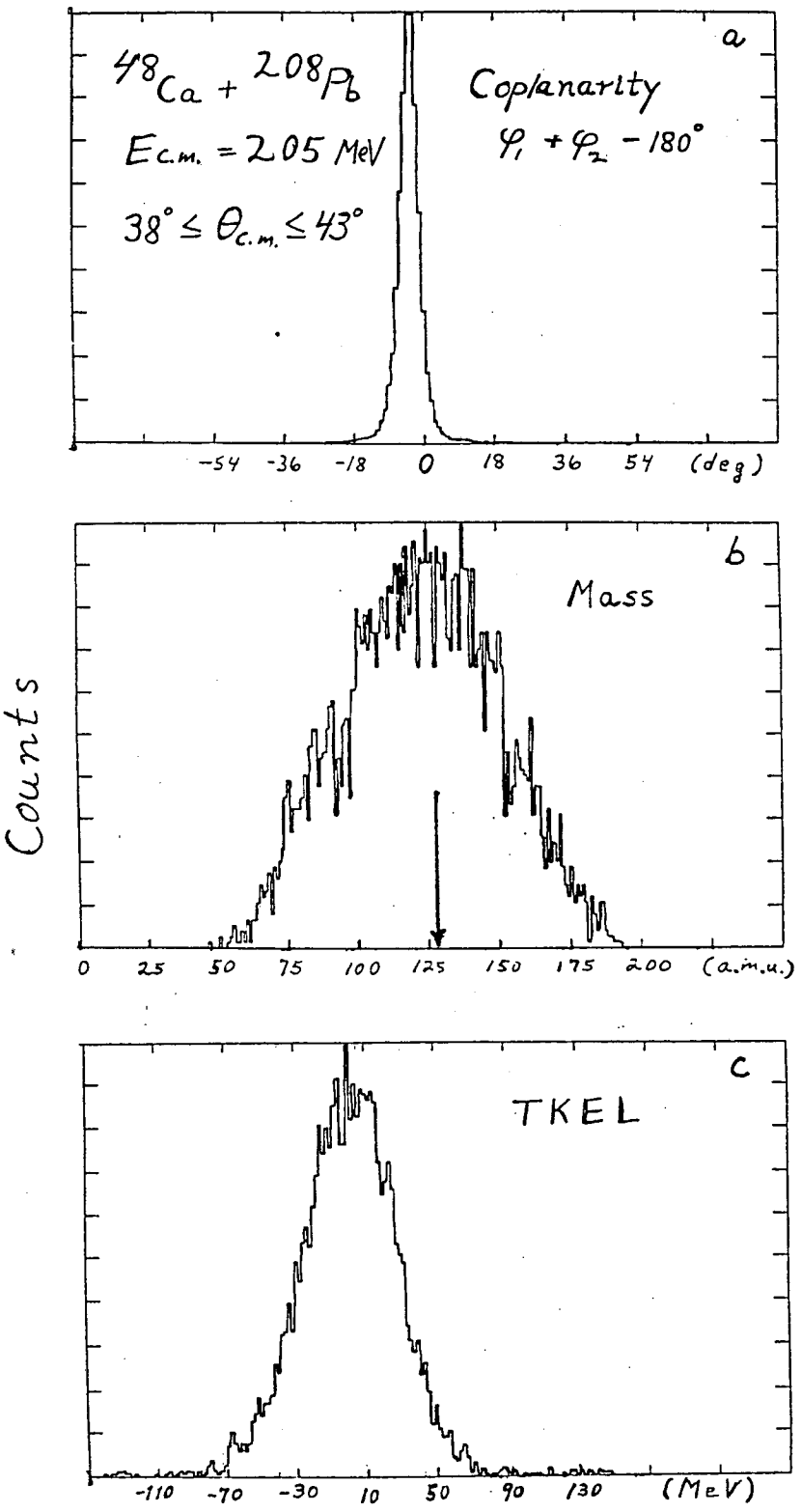
a
$^{48}Ca + ^{208}Pb$
$E_{c.m.} = 205$ MeV
$38° \leq \theta_{c.m.} \leq 43°$
Coplanarity
$\varphi_1 + \varphi_2 - 180°$
-54 -36 -18 0 18 36 54 (deg)
b
Mass
Counts
0 25 50 75 100 125 150 175 200 (a.m.u.)
c
TKEL
-110 -70 -30 10 50 90 130 (MeV)

Fig. 3

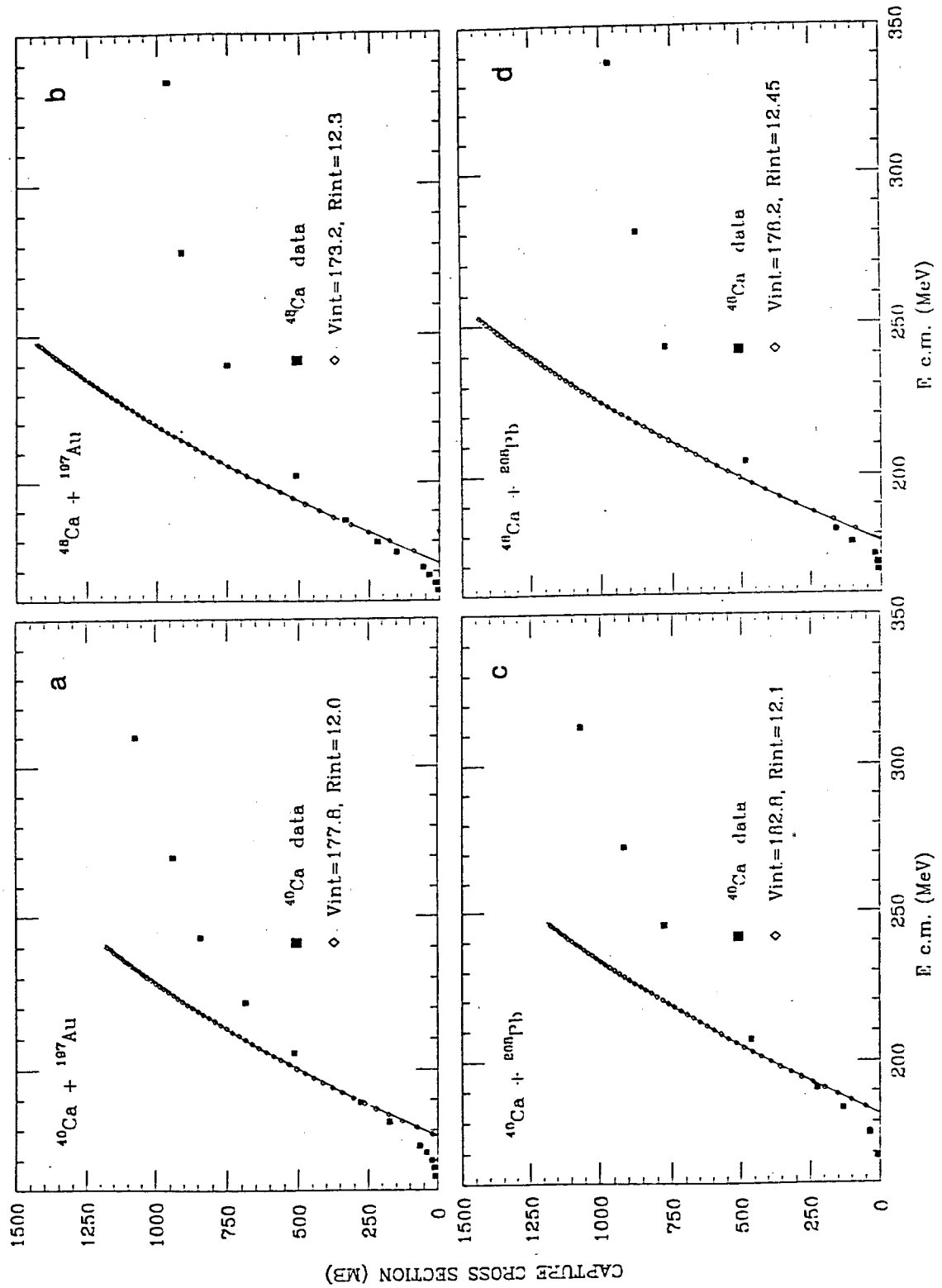
a
$^{40}Ca + ^{197}Au$
$^{40}Ca$ data
Vint=177.8, Rint=12.0
b
$^{48}Ca + ^{197}Au$
$^{48}Ca$ data
Vint=173.2, Rint=12.3
c
$^{40}Ca + ^{208}Pb$
$^{40}Ca$ data
Vint=182.8, Rint=12.1
d
$^{40}Ca + ^{208}Pb$
$^{40}Ca$ data
Vint=178.2, Rint=12.45
CAPTURE CROSS SECTION (MB)
E c.m. (MeV)
E c.m. (MeV)
0
250
500
750
1000
1250
1500
200
250
300
350

Fig. 4

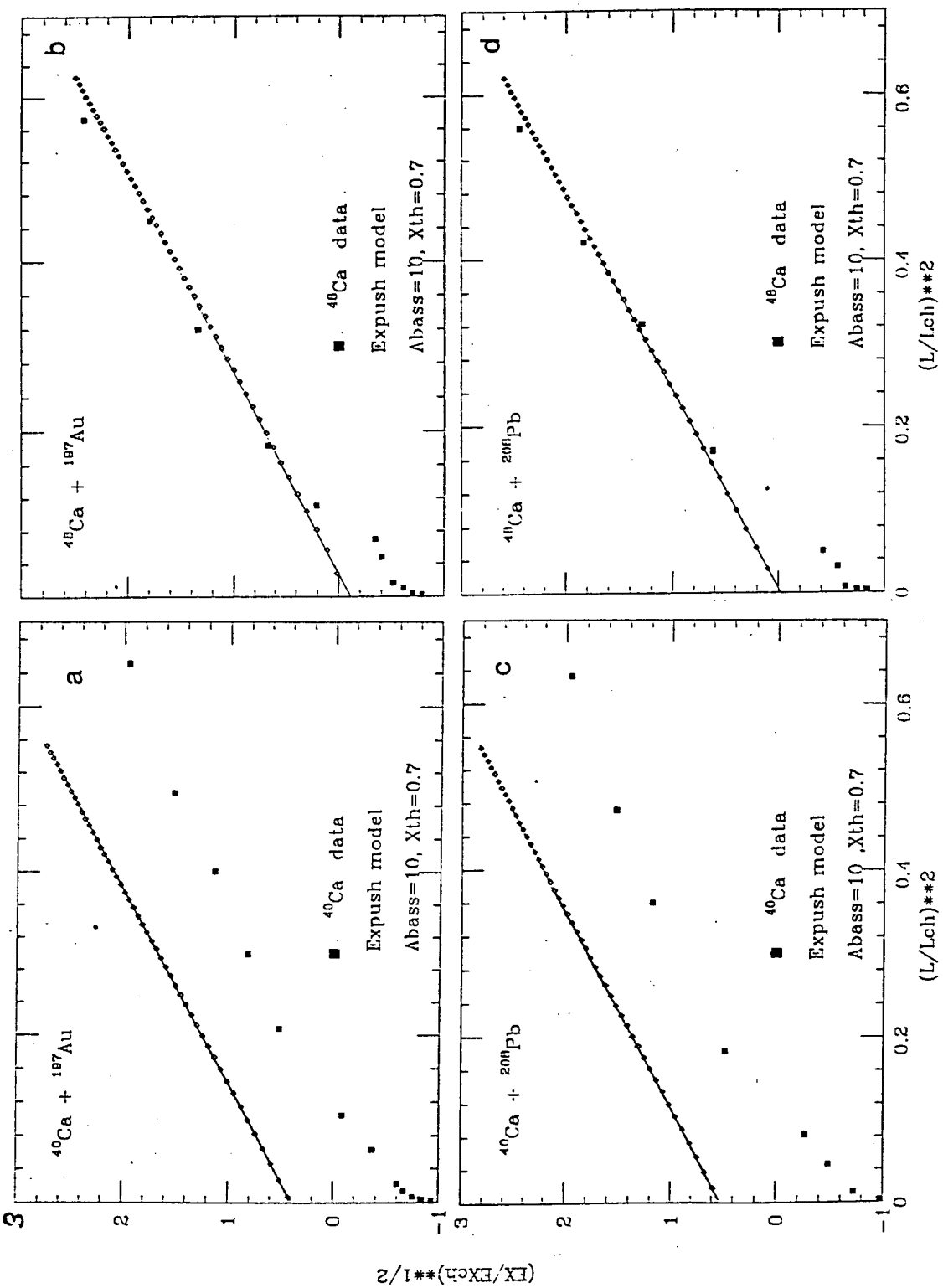
a
b
c
d
$^{40}Ca + ^{197}Au$
$^{40}Ca + ^{208}Pb$
$^{40}Ca$ data
Expush model
Abass=10, Xth=0.7
(EX/EXch)**1/2
(L/Lch)**2

Fig. 5

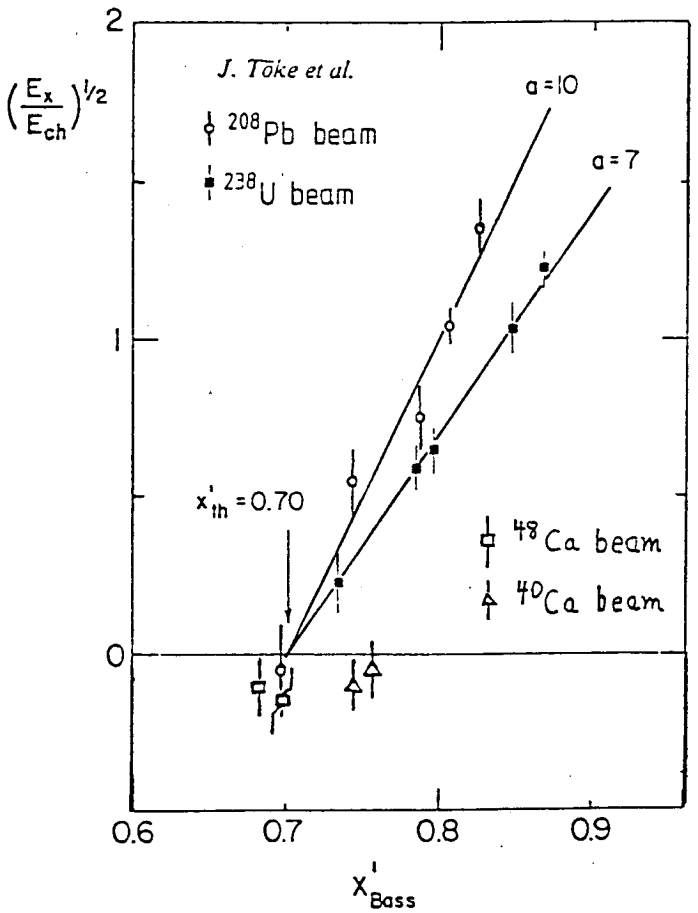
J. Töke et al.
$\left(\frac{E_x}{E_{ch}}\right)^{1/2}$
$^{208}$Pb beam
$^{238}$U beam
a=10
a=7
$x'_{th}$=0.70
$^{48}$Ca beam
$^{40}$Ca beam
2
1
0
0.6
0.7
0.8
0.9
$X'_{Bass}$

Fig. 6

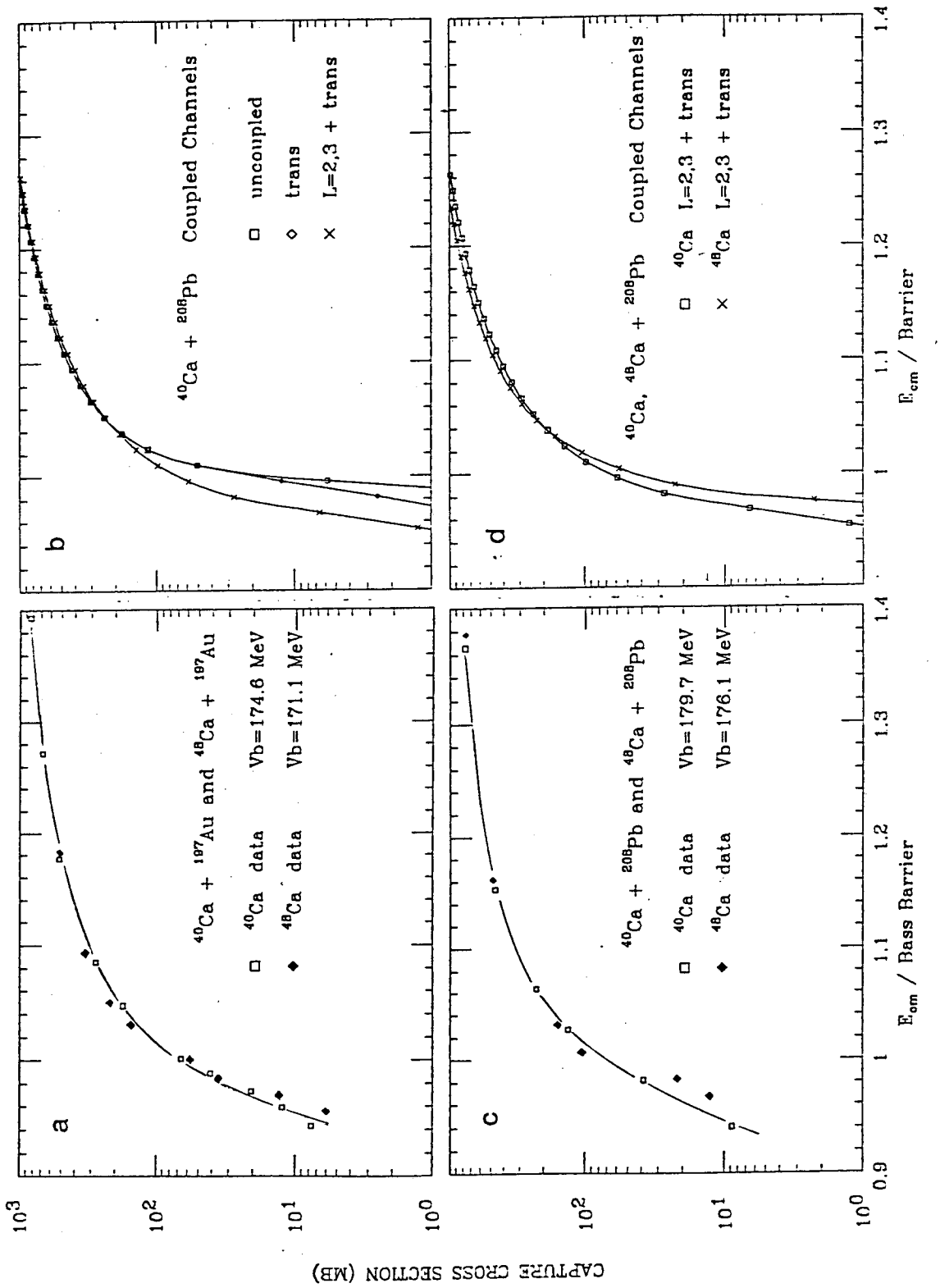
a
$^{40}$Ca + $^{197}$Au and $^{48}$Ca + $^{197}$Au
$^{40}$Ca data Vb=174.6 MeV
$^{48}$Ca data Vb=171.1 MeV
b
$^{40}$Ca + $^{208}$Pb Coupled Channels
uncoupled
trans
L=2,3 + trans
c
$^{40}$Ca + $^{208}$Pb and $^{48}$Ca + $^{208}$Pb
$^{40}$Ca data Vb=179.7 MeV
$^{48}$Ca data Vb=176.1 MeV
d
$^{40}$Ca, $^{48}$Ca + $^{208}$Pb Coupled Channels
$^{40}$Ca L=2,3 + trans
$^{48}$Ca L=2,3 + trans
CAPTURE CROSS SECTION (MB)
$E_{cm}$ / Bass Barrier
$E_{cm}$ / Barrier

Fig. 7

*LAWRENCE BERKELEY LABORATORY*
*TECHNICAL INFORMATION DEPARTMENT*
*UNIVERSITY OF CALIFORNIA*
*BERKELEY, CALIFORNIA 94720*